Solution Structure of a DNA Complex with the Fluorescent Bis-Intercalator TOTO Determined by NMR Spectroscopy[†,‡]

H. Peter Spielmann,[§] David E. Wemmer,[§] and Jens Peter Jacobsen*,[‖]

Department of Chemistry, Odense University, Odense M-5230, Denmark, and Structural Biology Division, Lawrence Berkeley Laboratory, and Department of Chemistry, University of California, Berkeley, California 94720

Received January 6, 1995; Revised Manuscript Received February 27, 1995[⊗]

ABSTRACT: We have used two-dimensional ^{1}H NMR spectroscopy to determine the solution structure of the DNA oligonucleotide d(5′-CGCTAGCG-3′)$_2$ complexed with the bis-intercalating dye 1,1′-(4,4,8,8-tetramethyl-4,8-diazaundecamethylene)bis[4-(3-methyl-2,3-dihydrobenzo-1,3-thiazolyl-2-methylidene)quinolinium] tetraiodide (TOTO). The determination of the structure was based on total relaxation matrix analysis of the NOESY cross-peak intensities using the program MARDIGRAS. Improved procedures to consider the experimental "noise" in NOESY spectra during these calculations have been employed. The NOE-derived distance restraints were applied in restrained molecular dynamics calculations. Twenty final structures each were generated for the TOTO complex from both A-form and B-form dsDNA starting structures. The root-mean-square (rms) deviation of the coordinates for the 40 structures of the complex was 1.45 Å. The local DNA structure is distorted in the complex. The helix is unwound by 60° and has an overall helical repeat of 12 base pairs, caused by bis-intercalation of TOTO. The poly(propylenamine) linker chain is located in the minor groove of dsDNA. Calculations indicate that the benzothiazole ring system is twisted relative to the quinoline in the uncomplexed TOTO molecule. The site selectivity of TOTO for the CTAG•CTAG site is explained by its ability to adapt to the base pair propeller twist of dsDNA to optimize stacking and the hydrophobic interaction between the thymidine methyl group and the benzothiazole ring. There is a 3000-fold fluorescence enhancement upon binding of TOTO to dsDNA. Rotation about the cyanine methine bonds is possible in free TOTO, allowing relaxation nonradiatively. When bound to dsDNA, the benzothiazole ring and the quinolinium ring are clamped by the nucleobases preventing this rotation, and the chromophore loses excitation energy by fluorescence instead.

Recent interest in nonradioactive detection of nucleic acids in gels has led to the synthesis and evaluation of new dyes that form highly fluorescent complexes with double-stranded DNA (dsDNA)[1] (Rye et al., 1992; Benson et al., 1993a,b). Prominent among these is the homodimeric thiazole orange dye TOTO [1,1′-(4,4,8,8-tetramethyl-4,8-diazaundecamethylene)bis[4-(3-methyl-2,3-dihydrobenzo-1,3-thiazolyl)-2-methylidene)quinolinium] tetraiodide] (Figure 1). It has been shown to bind very tightly to dsDNA, presumably via bis-intercalation. TOTO's effectiveness as a nucleic acid stain stems from its ability to form complexes that are stable under gel electrophoresis conditions and a large enhancement in fluorescence (>3000-fold) upon binding of the dye to dsDNA.

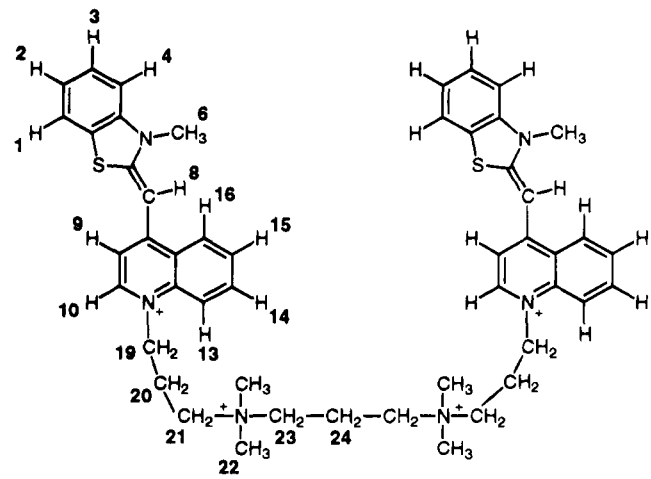

FIGURE 1: Structure of TOTO indicating the numbering scheme.

A previous ^{1}H NMR study of TOTO−DNA complexes (Jacobsen et al., 1995) indicated that binding does occur via bis-intercalation. Investigation of the dye binding to a number of dsDNA oligomers (from 4 to 12 base pairs in length) showed that complex formation is sequence selective. Line broadening arising from chemical exchange between

[†] This work was supported in part by National Institutes of Health Grant GM-43219 (D.E.W.), by Postdoctoral Fellowship GM-14966 (H.P.S.), through instrumentation grants from the U.S. Department of Energy, DE FG05-86ER75281, and the National Science Foundation, DMB 86-09305 and BBS 87-20134, and by the Director, Office of Biological and Environmental Research, General Sciences Division of the U.S. Department of Energy under Contract DE-AC03-76SF00098 (D.E.W.).

[‡] The coordinates of the final structures of the TOTO−DNA complex have been deposited in the Brookhaven Protein Data Bank. The structure has the PDB Tracking Number T5935 and ID code 108D.

* Corresponding author.

[§] Odense University.

[‖] University of California, Berkeley.

[⊗] Abstract published in *Advance ACS Abstracts,* June 15, 1995.

[1] Abbreviations: AMBER, assisted model building with energy refinement; DMSO, dimethyl sulfoxide; dsDNA, double-stranded DNA; EDTA, ethylenediaminetetraacetic acid; MARDIGRAS, matrix analysis of relaxation for discerning the geometry of an aqueous structure; MOPAC, molecular orbital package; NMR, nuclear magnetic resonance; NOE, nuclear Overhauser effect; NOESY, nuclear Overhauser effect spectroscopy; RANDMARDI, randomized MARDIGRAS; RMD, restrained molecular dynamics; TOCSY, total correlation spectroscopy; TOTO, 1,1′-(4,4,8,8-tetramethyl-4,8-diazaundecamethylene)bis[4-(3-methyl-2,3-dihydrobenzo-1,3-thiazolyl-2-methylidene)quinolinium] tetraiodide; TPPI, time-proportional phase incrementation.

0006-2960/95/0434-8542$09.00/0

various binding sites was observed for many sequences. However, sharp lines were obtained for oligomers containing the sequence CTAG. Variations on this sequence established that CTAG·CTAG is the optimal binding site for the dye. TOTO binds to this site with an affinity ca. 100 times higher than other possible sites in the oligomer and bis-intercalates at the C-T and A-G steps.

The charged alkyl−amino linker of TOTO resembles spermidine and spermine. The binding of these polyamines to dsDNA has been studied with different methods and has been found to be nonsequence selective (Wemmer et al., 1985; Padmanabhan et al., 1988, 1991; Braunlin et al., 1986). This suggests that the linker of TOTO contributes substantially to the binding affinity but probably not to the sequence selectivity in binding. Thus the observed sequence preference for the CTAG site must come primarily from interaction of the thiazole orange chromophores with the bases of the dsDNA. Here we describe the results of an NMR structural study of TOTO bound to the oligonucleotide d(CGCTAGCG)$_2$, which was undertaken to determine the structural basis for the sequence-selective binding and origin of the fluorescence enhancement. Such studies may ultimately also lead to new designs for analogs of TOTO which could have improved site selectivity and/or fluorescence properties.

The structure of this complex was determined using ^{1}H NMR. NOESY spectra were used to obtain interproton distance estimates using the RANDMARDI procedure (H. Liu, H. P. Spielman, D. E. Wemmer, and T. L. James, unpublished results), a variation of the MARDIGRAS complete relaxation matrix approach (Borgias & James, 1990; Borgias et al., 1990; Schmitz et al., 1992). Distance estimates derived using this approach were then used as restraints in molecular dynamics simulations (RMD). Since many contacts were observed between the TOTO and dsDNA, the resulting structures have fairly high resolution and allowed determination of local features in the dsDNA structure after TOTO binding.

MATERIALS AND METHODS

Sample Preparation. The oligonucleotide d(CGCTAGCG)$_2$ was purchased from DNA Technology, Aarhus, Denmark, and used without further purification. The numbering scheme for the double-stranded oligonucleotide is

```
5'-C1  G2  C3  T4  A5  G6  C7  G8 -3'
3'-G16 C15 G14 A13 T12 C11 G10 C9 -5'
```

TOTO is almost insoluble in water, and the complexes with dsDNA can therefore not be made by simple titration of the dsDNA with TOTO. Instead, TOTO was dissolved in DMSO-d_6 and added gradually with rapid stirring to an equimolar amount of the oligonucleotide dissolved in ca. 5 mL of water. The reaction mixture was lyophilized on a Speedvac concentrator (Savant) immediately following the addition. Lyophilizing twice from D_2O left no visible DMSO and no lines from DMSO-d_5 in the ^{1}H NMR spectrum. The TOTO complexes formed are stable in water solution. The concentrations of the dsDNA and the TOTO stock solutions were determined by UV spectroscopy using the extinction coefficients reported in the literature (Rye et al., 1992; Brown et al., 1991).

The NMR samples were prepared by dissolving the complexes in 0.5 mL of 10 mM sodium phosphate buffer (pH 7.0) and 0.05 mM Na EDTA. For experiments carried out in D_2O the solid complex, lyophilized twice from D_2O, was redissolved in 99.96% D_2O (Cambridge Isotope Laboratories). A mixture of 90% H_2O and 10% D_2O (0.5 mL) was used for experiments examining exchangeable protons. The sample was kept in an NMR tube under nitrogen. The final concentration of the complex was 3 mM.

NMR Experiments. All NMR experiments were performed on a Varian Unity 500 spectrometer at 25 °C unless otherwise indicated. NOESY spectra were acquired in D_2O using 1024 complex points in t_2 and a spectral width of 5000 Hz. A total of 512 t_1 experiments were recorded using the States phase cycling scheme (States et al., 1982). The residual signal from HOD was removed by presaturation. NOE buildups were obtained by collecting NOESY spectra with mixing times of 25, 50, 100, 150, and 200 ms with 96 scans acquired for each t_1 value. The NOESY spectra were obtained sequentially without removing the sample from the magnet. TOCSY spectra (Bax & Davis, 1985; Levitt et al., 1982) with mixing times of 30, 90, and 130 ms were obtained in the TPPI mode (Bodenhausen et al., 1984) using 1024 complex points in t_2 and 512 t_1 experiments with 64 scans each. Removal of the residual HOD signal was done by presaturation. The NOESY spectra in H_2O were acquired with a spectral width of 10 000 Hz in 2048 complex points using a pulse sequence where the last 90° pulse was replaced by a pulse containing a notch to suppress the solvent signal (P. C. Stein, H. P. Spielman, and J. P. Jacobsen, unpublished results). The acquired data were processed using Felix (version 2.1, Biosym Technologies, San Diego). The TOCSY and NOESY spectra were analyzed by conventional methods (Hare et al., 1983; Wüthrich, 1986).

Structure Calculations. The upper and lower diagonal part of each of the five assigned NOESY spectra was integrated separately with Felix, yielding a total of ten peak intensity sets. The RANDMARDI procedure (Liu et al., unpublished results) of the complete relaxation matrix analysis method, MARDIGRAS (Borgias & James, 1990; Borgias et al., 1990), was used to calculate interproton distance RMD bounds from the resulting integrated peak intensities. The RANDMARDI procedure was used to include the effects of experimental noise in the relaxation matrix calculations. RANDMARDI adds a random number from within a specified range to each input intensity used in a MARDIGRAS calculation. For the calculations performed on the TOTO−DNA complex a noise level of 1−5 times the integrated intensity of the smallest cross peak was used as the "noise" range. The dynamic range of observed cross-peak intensities was 1000. In the RANDMARDI procedure, 30 different intensity sets from each experimental data set were generated, and MARDIGRAS calculations were performed on all of them. Resulting distances were then averaged together to form one bounds file for each of the ten data sets. The bounds files from all of the mixing times are then combined into a single bounds file from which the RMD restraint file is generated. Upper and lower bounds were average interproton distances ± 1 standard deviation calculated from all of the MARDIGRAS runs. A complete description of the RANDMARDI theory and procedure will be given elsewhere (Liu et al., unpublished results).

MARDIGRAS uses internal calibrations when it iteratively fits the data to a model of the molecule. In particular, it resets the cytosine H5 to H6, the thymidine 5-methyl to H6,

and deoxyribose H2′ to H2″ interproton distances to the values assumed from the covalent geometries. NOE intensities for these known distances are used to normalize the NOE intensities in the model. The program does not reset proton distances within TOTO because these distances were intentionally left out of the reference file. The magnetization transfer for these protons is calculated and provides a check of how well the MARDIGRAS procedure is working. Good agreement between the actual and the experimentally determined distances indicates that the RANDMARDI procedure yields accurate interproton distances (see Table 1, discussion below).

The distance restraints obtained from the MARDIGRAS calculations were incorporated into an RMD procedure. The RMD and energy minimization calculations were performed using Discover (version 2.9.5) with modified AMBER forcefield potentials. The models were displayed using InsightII (version 2.3.0) (Biosym Technologies, San Diego). The TOTO was manually docked into a model of either A-form or B-form DNA. The NOE-derived distance restraints were applied, and the model was energy minimized. This was followed by 28 ps of restrained molecular dynamics at 600 K for 4 ps, followed by cooling to 200 K in 50 K steps of 3 ps each. The final structure was then energy minimized to a maximum derivative of 0.01 Å.

The pseudo-energy term used to enforce the distance restraints was

$$E_{\text{constr}} = \begin{cases} k_1(r - r_2)^2 & \text{when } r_2 > r \\ 0 & \text{when } r_3 \geq r \geq r_2 \\ k_2(r - r_3)^2 & \text{when } r_3 > r \end{cases}$$

where r_2 and r_3 are the upper and lower distance bounds determined from the cross-peak volumes and k_1 and k_2 are the force constants that could be independently adjusted for each restraint. An upper and lower bound force constant of 50 kcal/(mol Å^2) was assigned for all NOE-derived distance restraints. The width of the flat region of the potential well reflects the accuracy of a given constraint. An additional 22 distance restraints were included to enforce Watson–Crick hydrogen bonding throughout the calculations. Three hydrogen bonds were included for each of the six G-C base pairs and two hydrogen bonds for each of the A-T base pairs with lower and upper bounds of 1.7 and 2.1 Å, respectively.

Helix parameters were calculated with the program CURVES 3.1 (Lavery & Sklenar, 1988, 1989). The electronic and structure calculations on free TOTO were performed with the program MOPAC 93 (Stewart, 1993).

RESULTS

Spectral Analysis. The proton resonances of this TOTO complex have relatively narrow line widths, ca. 10 Hz, as narrow as observed for any of the TOTO–dsDNA complexes (Jacobsen et al., 1995). Observations of lines for just one DNA strand and one thiazole orange (TO) chromophore show that the TOTO complex has dyad symmetry. NOESY and TOCSY spectra were used to assign DNA and TOTO resonances. Parts of the NOESY spectra are given in Figures 2 and 3.

The NOESY spectra in Figures 2 and 3 exhibit the characteristic features of dsDNA sequential connectivities

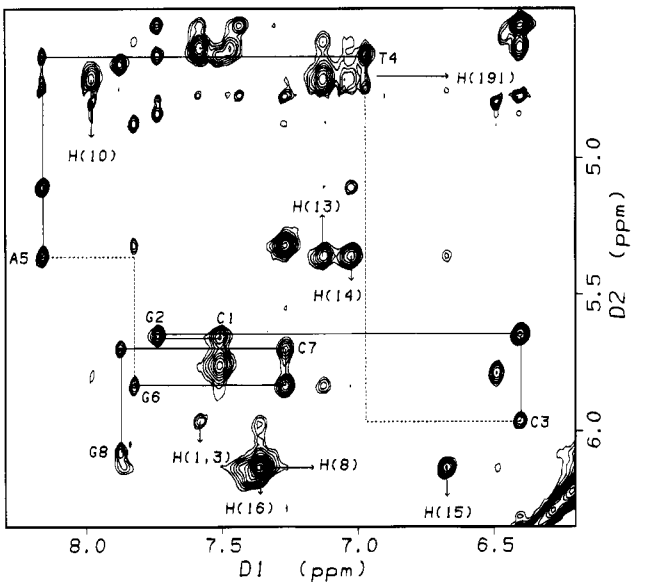

FIGURE 2: The H1′ to aromatic part of the 150 ms NOESY spectrum of the TOTO complex. The sequential H1′–H6/H8–H1′ connectivity pathway is indicated by a solid line. The interrupted connectivities at the 5′-C3pT4-3′ and 5′-A5pG6-3′ base pair steps due to intercalation sites are indicated by a dotted line. A few of the observed cross peaks between TOTO and the oligonucleotide are also marked. It is noteworthy that the cross peak between TOTO H15 and A5 H1′ has a measured volume which is approximately 100 times smaller than the observed cross peaks between TOTO H8 and H16. This demonstrates the large dynamic range and precision of the measured intensities obtainable from these spectra.

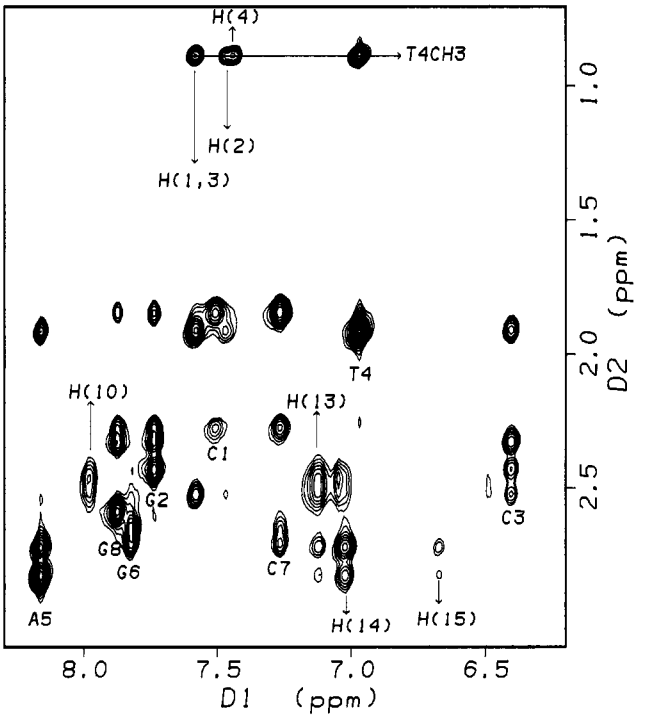

FIGURE 3: H2′/H2″ to aromatic part of the 150 ms NOESY spectrum of the TOTO complex. The assignments of the H6/H8 resonances for the various nucleotides are indicated together with the resonances of the thymidine methyl protons and some of the TOTO protons. As shown, TOTO H13, H14, and H15 resonances all have cross peaks to A5 H2′ and H2″, but TOTO H14 has by far the most intense ones. This is a demonstration of the degree of detailed information obtainable from this spectrum.

from aromatic H6/H8 protons to both intra- and interresidue H1′ and H2′/H2″. However, the sequential connectivities

are interrupted at the 5′-C3pT4-3′ and 5′-A5pG6-3′ base pair steps. This is clear evidence of bis-intercalation. Figure 2 also includes a few of the observed cross peaks between TOTO and the oligonucleotide. Interruption of the sequential NOE connectivities is also observed in the cross-peak pattern of the methyl group of T4 for which the peak to C3 H6 is missing. This is shown in the part of the NOESY spectrum given in Figure 3. Aromatic (H6, H5, H8, and H2) and deoxyribose proton (H1′, H2′, H2″, H3′, H4′, and H5′/H5″) resonances of dsDNA in the complex were assigned in the conventional way (Hare et al., 1983; Wüthrich, 1986). The assignments are given in Table 3.

The NOESY spectrum of the complex in H_2O shows the normal Watson−Crick NOE connectivity pattern, again interrupted at the 3−4 and 5−6 base pair steps (Wüthrich, 1986). Chemical shift values of labile protons are included in Table 3. Furthermore, the spectra in H_2O contain distinct cross peaks between the thymidine imino proton (T4 H3) and the amino protons of the base-paired adenosine (A13 H6). These peaks are absent in normal dsDNA at room temperature due to exchange. The lowering of the exchange rates of the adenosine amino protons on complex formation is a consequence of the bis-intercalation. Similarly, exchange cross peaks between water and the thymidine imino protons are absent at room temperature, and only very small ones are observed for the G6/G14 imino protons. The G2/G10 imino protons yield an exchange cross peak to water of normal intensity.

The internal NOE connectivities in the chromophore of TOTO are a distinct feature of the NOESY spectra of the complex. Cross-peak patterns connect {H16−H15−H14−H13}, {H8−$CH_3$6−H4−H3−H2−H1}, and {H9−H10}, respectively. A very strong cross peak between H8 and H16 and a cross-peak pattern connecting H10−H19−H13 establish the assignments of the individual protons and conformation of the TOTO ligand. Resonances in the linker of TOTO were assigned by combined use of TOCSY and NOESY cross peaks. Chemical shift values of TOTO in the complex are given in Table 3. The conformation of free TOTO in a DMSO-d_6 solution has been studied by Glazer and coworkers (Rye et al., 1992). On the basis of the cross-peak pattern in the NOESY spectrum, they showed that the relative conformation of the two ring systems in each chromophore is that indicated in Figure 1. We have found exactly the same cross-peak pattern for TOTO bound to dsDNA. The relative conformation of the aromatic ring systems about the cyanine methine bonds in the chromophores is therefore unaffected by intercalation into dsDNA.

Although the regular sequential path in NOESY spectra is interrupted at the intercalation sites, there is a sequential path from the 5′ end to the 3′ end of each strand of the dsDNA by including connectivities from protons on the oligonucleotide to protons on TOTO. It is also possible to "walk" across the two strands through the dye. There is only a single possible path of each type. This conclusively defines the intercalation site.

Cross peaks in the NOESY spectra unambiguously show that the poly(propylenamine) linker is positioned in the minor groove. This is demonstrated by a large number of cross peaks: The H2 of the adenines gives cross peaks to the linker protons H21, H22, and H23, the H1′ of the adenines to the linker protons H21, H22, and H23, and the linker H19 protons to the H1′ of the guanines in the intercalation site.

Table 1: Covalently Determined Interproton Distances (Å) in TOTO and a Comparison between Actual Values and Values Obtained from MARDIGRAS Calculations

atom	pair	actual values[a]	lower bounds[b]	upper bounds[b]	width[b]	violations
H3	$CH_3$6	5.44	3.97	5.27	1.30	0.17
H4	$CH_3$6	3.04	2.75	2.85	0.10	0.17
H9	H16	4.86	3.35	4.88	1.53	
H10	H13	4.81	3.43	5.02	1.59	
H15	H13	4.27	3.11	4.15	1.04	0.12
H9	H10	2.40	2.23	2.41	0.18	
H16	H15	2.44	2.32	2.46	0.14	

[a] Obtained from MOPAC calculations. [b] Obtained from MARDIGRAS calculations and derived from the average distance ± 1 standard deviation.

The H4′ of the adenines and the guanines in the binding site also shows cross peaks to linker protons.

Structure Calculation. More than 400 NOE cross peaks were observed in the NOESY spectrum obtained with a mixing time of 200 ms. Some of them resulted predominantly from spin diffusion and were consequently not observed in NOESY spectra with shorter mixing times. The accuracy of the integration of some cross peaks was hampered by spectral overlap. Such cross peaks were therefore not included in the MARDIGRAS calculations. The integrated intensities from 193 NOESY cross peaks were used in the total relaxation analysis. Because of the symmetry in the complex, the number of cross peaks used in the MARDIGRAS calculations was actually doubled to 386. Of these, 352 cross-peak intensities corresponded to interproton distances that are not covalently fixed in either the dye or DNA in the complex. Integrations of the cross peaks in the five NOESY spectra used were done separately for each side of the diagonal. This yielded a total of 10 sets of measured NOE intensities that were converted to distance restraints using the RANDMARDI procedure. Not all cross peaks were present at all mixing times. The absence of a measured cross peak at some of the mixing times was taken into account during the statistical analysis of the results generated by the RANDMARDI procedure (see above). Cross-peak integrals that corresponded to fixed distances in the dsDNA were not converted into distance restraints for use in the RMD simulations. The calculations returned 362 interproton distances based on the 386 NOE cross peaks. The reliability of these distance restraints was examined by comparing the covalently fixed distances in TOTO to the distances obtained from the MARDIGRAS calculations (Table 1). The almost complete agreement between the actual and the experimentally determined distances indicates that the RANDMARDI procedure yields accurate interproton distances. The MARDIGRAS calculations were performed with various values of the correlation time for the complex in the range from 2 to 5 ns. The results were fairly insensitive to the actual value, and a correlation time of 3.75 ns was chosen for the final calculations.

The bounds for use in RMD simulations were determined by combining the results from all of the individual MARDIGRAS calculations performed during the RANDMARDI procedure into one set. The distance bounds were calculated individually for each proton pair corresponding to a NOESY cross peak included in the RANDMARDI calculations. Each individual restraint was generated from the average distance calculated for that proton pair from the MARDIGRAS

Table 2: Number of Distance Restraints Used in the RMD Dynamic Calculations of the TOTO Complex[a]

	intraresidue						
	intrasugar	base−sugar	total	interresidue		dye−DNA	
C1	6	4	10	C1−G2	5[b]	C3−TOTO	12
G2	4	5	9	G2−C3	8[b]	T4−TOTO	5
C3	5	6	11	C3−T4	0	A5−TOTO	18
T4	0	1	1	T4−A5	6[c]	G6−TOTO	11
A5	16	6	22	A5−G6	0		
G6	10	7	17	G6−C7	8		
C7	2	5	7	C7−G8	6		
G8	6	5	11				
total	49	39	88	total	33	total	46

[a] The restraints were derived from MARDIGRAS calculations unless otherwise stated. The 181 NOE connectivities (including 14 intraresidue dye distance restraints not given in the table) gave a total of 362 symmetry-related distance restraints; 22 distance restraints ensuring Watson−Crick base pairing were also included in the calculations. [b] One of the restraints was derived directly from inspection of the spectra and used with loose bounds. [c] Three of the restraints were derived directly from inspection of the spectra and used with loose bounds.

calculations, ±1 standard deviation calculated for that proton pair. No symmetry was enforced during the RANDMARDI procedure. The bounds for symmetry-related restraints was calculated by averaging the symmetry related upper and lower bounds for use in the RMD calculations. No additional symmetry was enforced during the RMD calculations. An additional 0.2 Å was added to all of the upper bounds for all of the restraints used in the RMD simulations. Table 2 gives a summary of the distance restraints used in the RMD calculations. The range of differences between the upper and lower bounds for the 362 NOE-derived restraint bounds used (cf. Table 2) was between 0.3 and 2.7 Å with an average flat well potential width of 1.26 Å. This range between the upper and lower bounds represents the accuracy of the restraint calculated from the NOESY data. Weak NOESY cross peaks that arose primarily from spin diffusion had the greatest difference between their upper and lower bounds.

NOESY spectra obtained in H_2O showed that normal Watson−Crick hydrogen bonding was present for all of the base pairs in the complex, justifying inclusion of 22 hydrogen bond distance restraints. An additional ten restraints with loose bounds were derived by inspection of the spectra for a total of 384 restraints. Twenty final structures each were generated for the TOTO complex starting with dsDNA in B-form and A-form. All the structures converged to the same conformation. The root-mean-square (rms) deviation of the coordinates of the 40 structures was 1.45 Å. The resulting total violations summed to 6.2 Å for the A-form starting structure and to 7.9 Å for the B-form starting structure. No violations greater than 0.25 Å and only two greater than 0.2 Å were found in any of the structures. Different views of the calculated structures are given in Figures 4−7.

Helix Parameters. Helical parameters for the 40 final structures were thoroughly analyzed with the program CURVES 3.1 (Lavery & Sklenar, 1988, 1989). The CURVES algorithm allows the determination of local structural parameters and the overall helical axis for irregular nucleic acid structures. The output of CURVES includes "global helical parameters" defined relative to the global helix axis and "local helical parameters" defined relative to local helix axes at each base pair. Plots of some of the global helical parameters for the averages and standard deviations for the TOTO complex are shown in Figure 8. The structural parameters for canonical A-DNA and B-DNA are included in Figure 8 for comparison.

DISCUSSION

Description of the Structure. The structure of the TOTO−dsDNA complex reveals that TOTO bis-intercalates in the CTAG•CTAG site with the benzothiazole ring system sandwiched between the pyrimidines and the quinolinium ring system between the purines. The *N*-methyl group on the benzothiazole is centered in the major groove. The linker between the two chromophores is positioned in the minor groove crossing from one side of the groove to the other. This probably introduces van der Waals contacts between the linker chain *N*-methyl groups and the walls of the groove. The length of the linker exactly matches the dsDNA

Table 3: Chemical Shift Values of the TOTO Complex with $d(CGCTAGCG)_2$ at 25 °C Compared to Free dsDNA Given in Parentheses[a]

	C1	G2	C3	T4	A5	G6	C7	G8
H8/H6	7.52 (7.67)	7.74 (8.01)	6.41 (7.46)	6.97 (7.42)	8.16 (8.24)	7.83 (7.71)	7.27 (7.31)	7.88 (7.95)
H5/CH_3/H2	5.76 (5.95)		4.50 (5.41)	0.89 (1.71)	7.05 (7.40)		5.32 (5.35)	
H1′	5.66 (5.82)	5.66 (5.98)	5.98 (6.00)	4.62 (5.63)	5.36 (6.05)	5.84 (5.73)	5.70 (5.78)	6.07 (6.17)
H2′	1.85 (2.03)	2.34 (2.74)	1.92 (2.08)	1.92 (2.15)	2.84 (2.76)	2.63 (2.52)	1.85 (1.89)	2.60 (2.62)
H2″	2.25 (2.47)	2.44 (2.79)	2.52 (2.53)	1.92 (2.46)	2.72 (2.90)	2.74 (2.62)	2.28 (2.35)	2.33 (2.39)
H3′	4.62 (4.74)	4.82 (5.02)	4.58 (4.78)	4.62 (4.90)	5.10 (5.06)	4.87 (4.97)	4.78 (4.80)	4.65 (4.68)
H4′	4.00 (4.11)	4.23 (4.40)	4.05 (4.27)	4.15 (4.17)	4.27 (4.42)	4.57 (4.38)	4.16 (4.16)	4.15 (4.18)
H5′	3.67 (4.75)	3.89 (4.14)	4.01 (4.27)	4.12 (4.11)	4.09 (4.17)	4.41 (4.21)	4.01 (4.12)	4.05 (4.08)
H5″	3.67 (4.75)	4.01 (4.04)	4.24 (4.21)	4.04 (4.11)	3.92 (4.09)	4.00 (4.21)	4.20 (4.21)	4.15 (4.08)
H1/H3		12.76 (13.05)		13.63 (13.79)		12.03 (12.78)		−
H4/H6	−		7.95 (8.30)		7.32 (−)		8.21 (8.36)	
H4/H6	−		6.58 (6.59)		6.72 (−)		6.44 (6.49)	

TOTO		TOTO		TOTO		TOTO	
H1	7.58	H9	6.50	H19′	4.15	$CH_3$22	3.28
H2	7.47	H10	7.98	H19″	4.70	H23′	3.41
H3	7.59	H13	7.14	H20′	2.5[b]	H23″	3.50
H4	7.44	H14	7.03	H20″	2.5[b]	H24′	2.5[b]
$CH_3$6	3.61	H15	6.68	H21′	3.62	H24″	2.5[b]
H8	6.13	H16	7.37	H21″	3.71		

[a] The values are given relative to the HOD signal at 4.78 ppm. Hydrogen-bonded amide protons are underlined. [b] Overlapping resonances at 2.5 ppm.

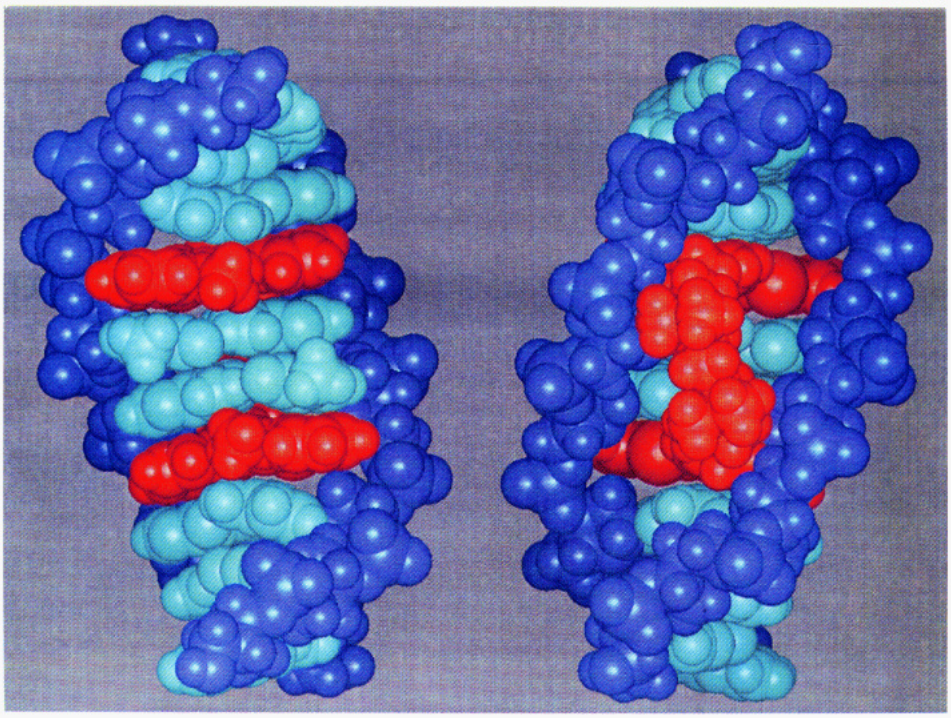

FIGURE 4: Structure of the TOTO−DNA complex looking into the minor groove (left) and the major groove (right). The TOTO molecule is shown in red, the nucleobases are in light blue, and the sugar−phosphate backbones are in dark blue.

structural requirements to fulfill nearest neighbor bis-intercalation. The sulfur atoms of the benzothiazoles are completely hidden from solvent and contact the O4′ of the thymidines.

In the complex the TOTO chromophores extend across the dsDNA helix. T4 and T12 unstack from A5 and A13 and move into the major groove to maximize van der Waals contacts with the benzothiazole ring of TOTO (Figure 7). The thymidine methyl groups are positioned right on top of the benzothiazole ring of TOTO. The observed imino proton cross peaks including the cross peaks to the adenine amino protons prove the existence of normal Watson−Crick base pairing in the intercalation site. So even though the thymidines are unstacked from the neighboring adenines, the base pairings of the thymidines with the complementary adenines do not appear to be appreciably disturbed.

NMR-derived restraints are short range in nature, and some helical parameters are better defined by the experimental data than others. In addition, the anisotropic distribution of observable interproton contacts by NMR in free dsDNA (largely confined to the ribbon of the sugar−phosphate backbone) defines some helical parameters poorly. In the case of the TOTO complex, there are a large number of NMR-derived restraints in the center of the helix due to the presence of the ligand. These TOTO−DNA contacts are fairly isotropic and therefore lock down the conformation for the central four base pairs of the complex. A 2-fold symmetry of the parameters about the center of the helix is evident and consistent with the nature of the complex.

Chemical Shifts. The chemical shift values of the dsDNA protons at the binding site in the TOTO complex reflect intercalation of the aromatic chromophores. Compared to the free dsDNA, the T4 $CH_3$6 protons are shifted 0.8 ppm upfield. This is in agreement with the structure of the complex that shows that this methyl group is positioned exactly above the benzothiazole ring (Figure 7) and thus exposed to a large ring current effect. Similar strong shifts are observed for T4 H1′, T4 H2″, A5 H1′, A5 H2″, C3 H6, and T4 H6, consistent with the positions of these protons above or below a ring system of the intercalating chromophore. It is commonly expected that intercalation imposes a large shift (~0.5 −1 ppm) (Assa-Munt et al., 1985a,b) on imino proton resonances adjacent to the binding site. However, this is only observed in the case of G6 H1 while T4 H3 remains almost unaffected by the intercalation of TOTO. The structure explains this observation since it shows that the T4 H3 proton is positioned above the methine group right next to the aromatic ring system. These protons are therefore not influenced by a ring current effect (Figure 7).

Helix Parameters. There are three major categories of helical parameters: axis−base pair, intra−base pair, and inter−base pair parameters (Dickerson et al., 1989). These parameters are discussed for the TOTO complex with respect to the calculated global helix axis below. However, the parameters reported for the terminal base pairs of the complex are probably less reliable because of dynamic processes and are included only for completeness. The deviation of the structures and calculated helical parameters from symmetry found for the complex spectroscopically reflects the level of uncertainty in the data.

(*A*) *Axis−Base Pair Parameters.* *X*-axis displacement in the complex is essentially that of B-DNA within the standard deviation calculated for the structures. All base pairs in the complex exhibit a non-zero *Y*-axis displacement. There is a 5′- to 3′- trend of negative to positive displacement for the central four base pairs that form the TOTO intercalation site. A C_2 operation about the center of symmetry gives essentially the same results counting along the other strand. The inclination for the central six base pairs around the intercalation site for the complex is centered around the value for B-DNA with evident C_2 symmetry. There is a discontinuity in the trend at the T4 to A5 base step. The tip angle starts positive and changes steadily to a negative value in a 5′−3′ direction across the thiazole orange monomer binding

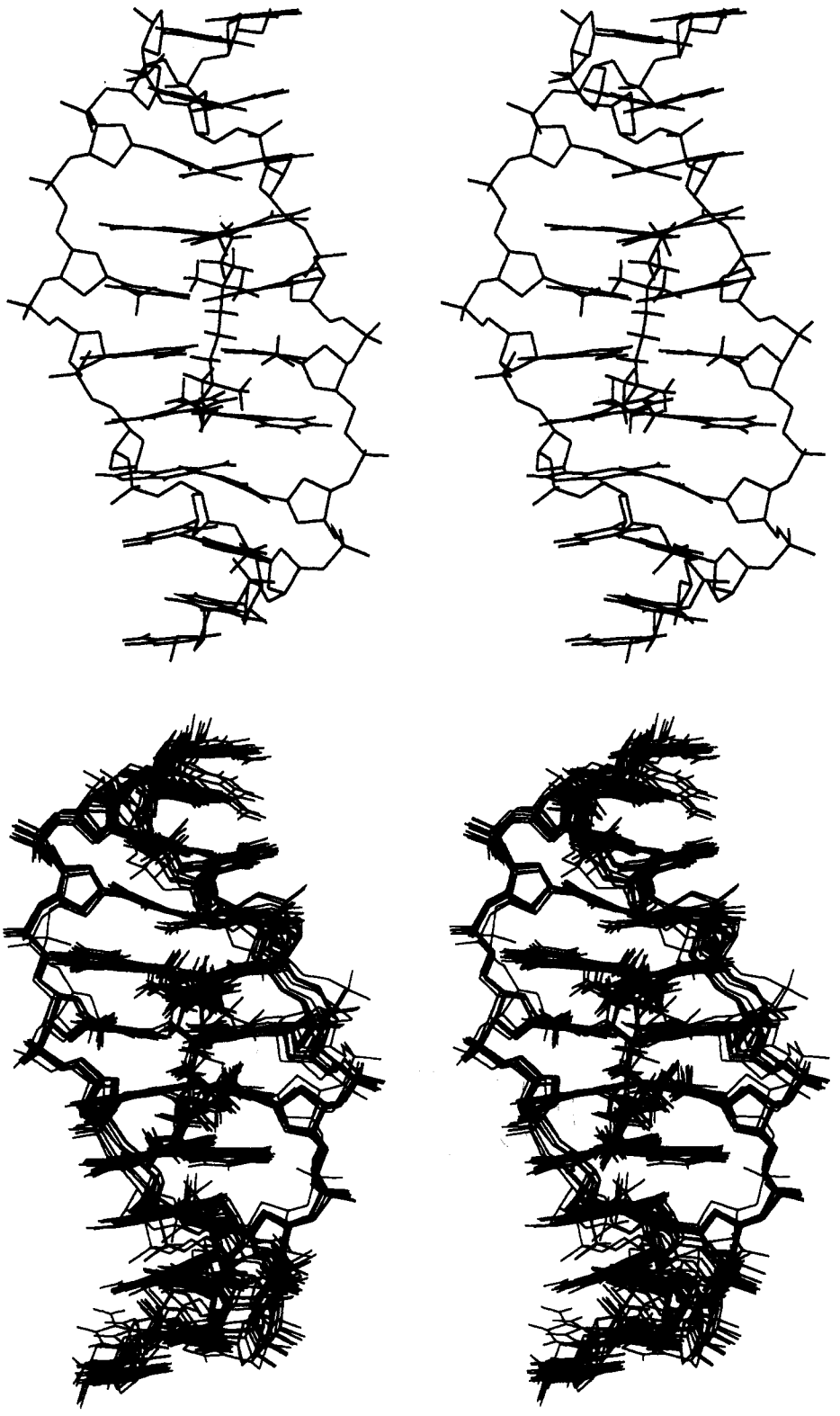

FIGURE 5: Stereoview of the stick plot of the structure of the TOTO−DNA complex. Deoxyribose protons have been omitted for clarity. (Top) One of the calculated structures. (Bottom) A superposition of 10 of the 40 structures obtained by RMD calculations.

site. A C_2 operation about the center of symmetry gives essentially the same result, counting along the other strand. The two chromophores of TOTO are not exactly coplanar with respect to each other, and the dsDNA probably accommodates for this distortion by altering the tip angle to maintain an overall linear structure.

(B) Intra−Base Pair Parameters. The calculated parameters for shear, stretch, stagger, and opening are mostly determined by the TOTO−DNA base NOEs in the case of the central four base pairs of the complex. The shear changes from positive to negative across the intercalation sites, compensating for the intercalation of the TOTO chromophores, returning to B-form values at the ends of the helix. As with the tip angle, there appears to be no net shear introduced into the overall complex. The stretch is essentially that of B-form DNA. The stagger is close to the

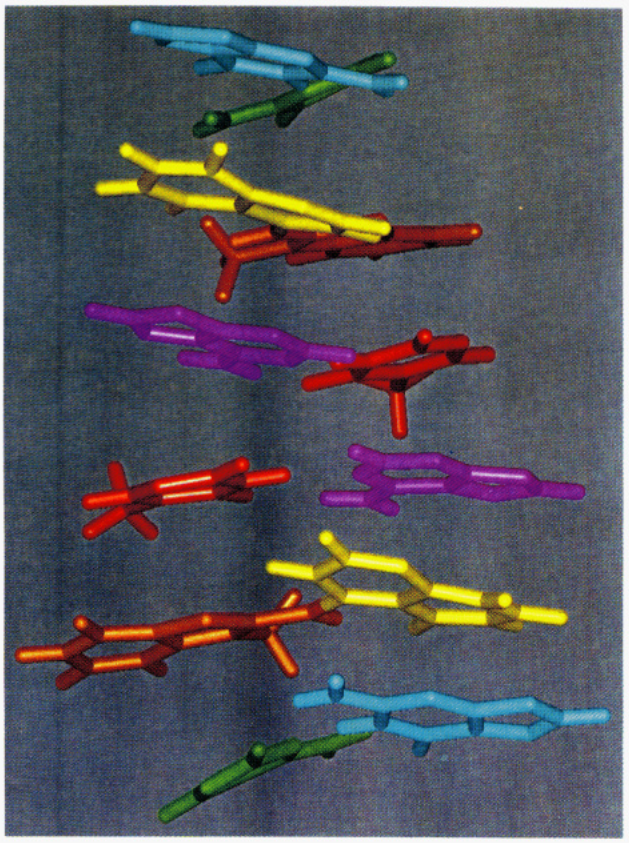

FIGURE 6: Stacking of the TOTO chromophore in the CpT·GpA binding site viewed from the side. Only the nucleobases are shown. The following color scheme has been used: the benzothiazole group of the TOTO chromophore, orange; the quinolinium group of the TOTO chromophore, yellow; the cytidine base, green; the thymine base, red; the guanine base, light blue; the adenine base, magenta.

normal A-DNA and B-DNA range. Base opening is confined to a range of ±10° symmetrically disposed around the central T4-A5 base step. The large deviations in the buckle from the normal A- and B-DNA value of 0° are a direct consequence of the intercalation of the TOTO chromophores. The dsDNA distorts by increasing buckle to maximize van der Waals contacts with the chromophores (Williams et al., 1992). The symmetry of the binding site is evident in the relative sign and distribution of the buckle across the TOTO binding site. The propeller twist varies symmetrically across the TOTO binding site in response to the inherently nonplanar chromophore of the TOTO. The chromophores are twisted about the quinoline−C8−thiazole bonds. MOPAC calculations indicate that the free chromophore adopts a conformation where the plane of the benzothiazole is 47° relative to the plane of the quinoline. The bound chromophore is found to have an angle of 22° between the two planes of the chromophore. The decrease of this angle is due to the clamping of the TOTO by the dsDNA in the complex. A change from 47° to 22° does not represent a large energy change since the MOPAC calculations show that the cyanine methine bond is rather flexible.

(C) Inter−Base Pair Parameters. The roll, slide, shift, and twist in regular A-DNA and B-DNA conformations are essentially zero. These parameters show large and correlated changes from the equilibrium values in the TOTO complex.

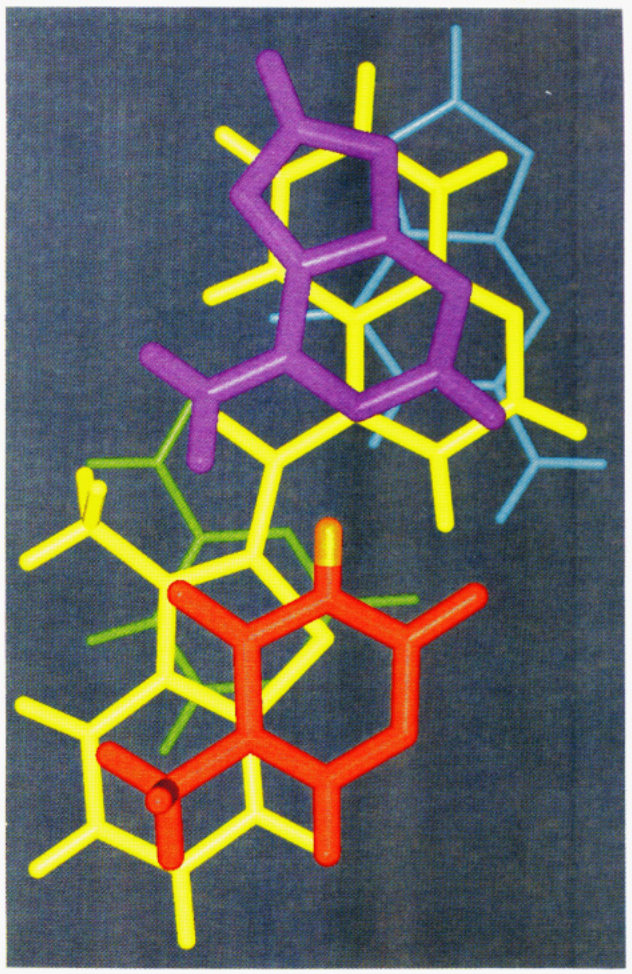

FIGURE 7: Stacking of the TOTO chromophore in the CpT·GpA binding site viewed down the helix axis. Only the nucleobase and the TOTO chromophores are shown. The following color scheme has been used: the TOTO chromophore, yellow; the cytidine base, green; the thymine base, red; the guanine base, light blue; the adenine base, magenta. The thymidine H3 is highlighted in orange.

There are shifts for the two intercalation sites with opposite signs that cancel each other in terms of the overall helix. The slide exhibits correlated and compensatory changes for the (G2-C3) and (C3-T4) base pair step to accommodate the dye intercalation. The rise for the (G2-C3) and (G6-C7) base pair steps flanking the intercalation step is 3.6 Å, exactly that of B-DNA. The (C3-T4) and (A5-G6) base pair steps have a rise of between 6.0 and 6.7 Å, reflecting the intercalation of the TOTO chromophores. The central (T4-A5) base pair step has a smaller rise of 2.4 Å, which is probably a consequence of the large and opposite change in buckle going from the (T4-A13) to (A5-T12) base pairs. The helix was found to be ~31 Å long. The two base pair steps flanking the intercalation sites exhibit a negative roll, while the central (T4-A5) base pair step has a positive roll. Positive roll opens the angle between base pairs toward the minor groove, resulting in a bend into the major groove, while a negative roll results in a bend into the minor groove. The central (T4-A5) base pair is clamped between the two thiazole orange chromophores, and to maximize the van der Waals contacts, the bases roll to open the minor groove. Because of the increased propeller twist induced by the chromophores, the second and third base pairs show a negative roll at these steps. There is no overall bend induced in the helix axis by these different rolls because they

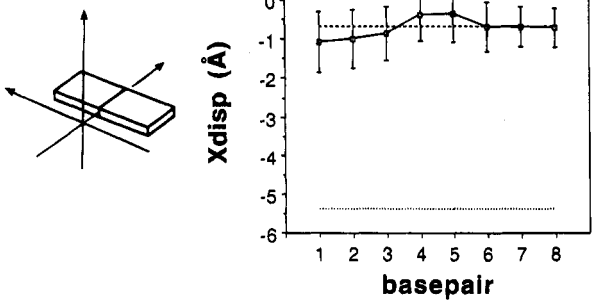
Xdisp (Å)
basepair

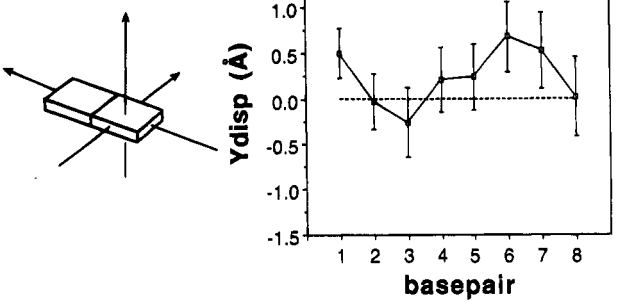
Ydisp (Å)
basepair

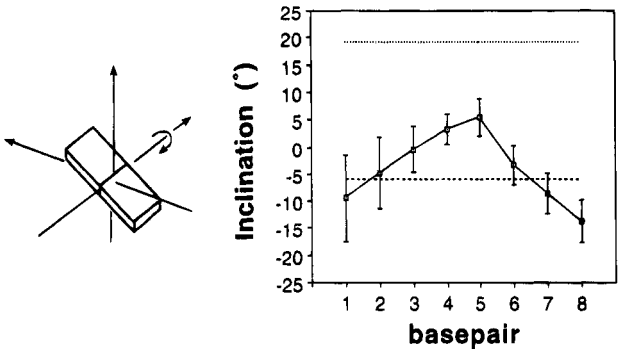
Inclination (°)
basepair

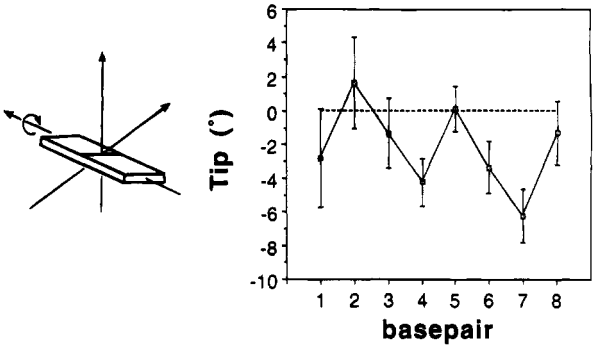
Tip (°)
basepair

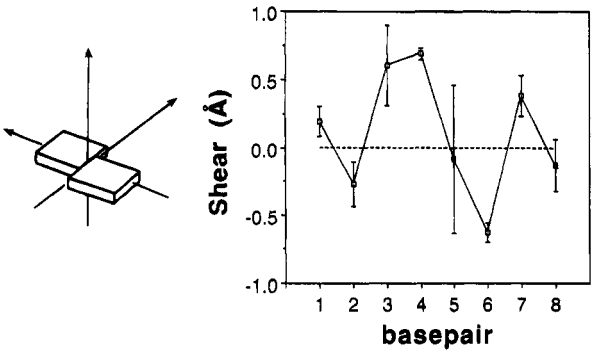
Shear (Å)
basepair

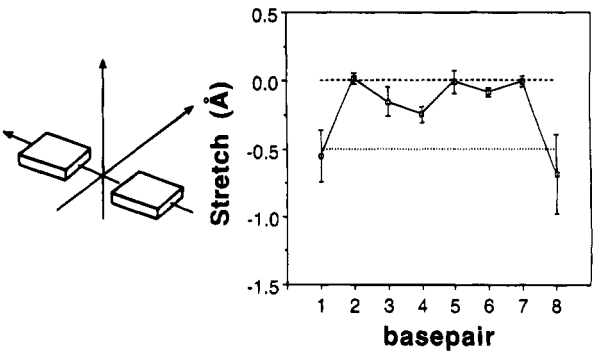
Stretch (Å)
basepair

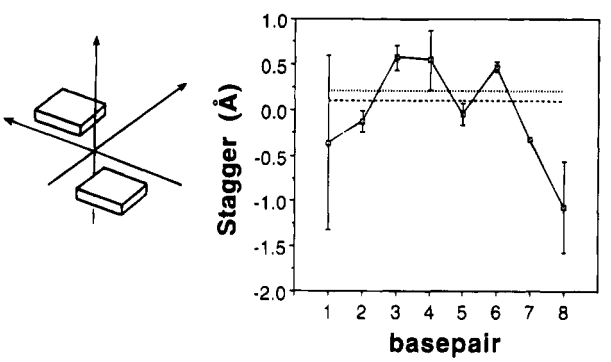
Stagger (Å)
basepair

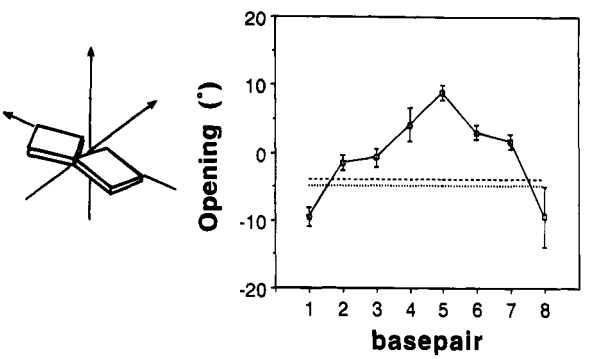
Opening (°)
basepair

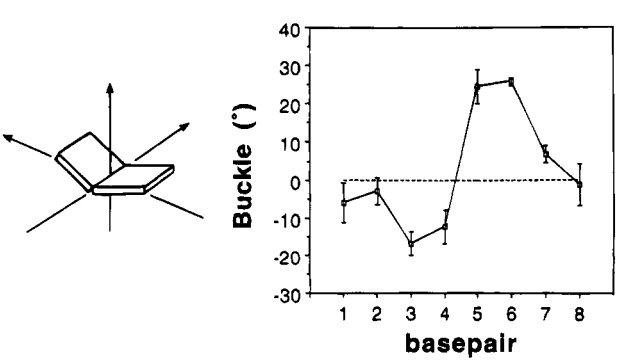
Buckle (°)
basepair

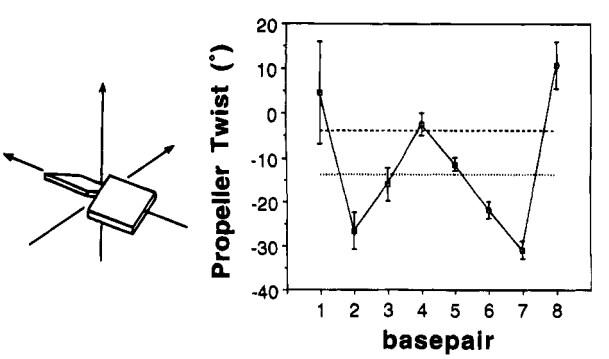
Propeller Twist (°)
basepair

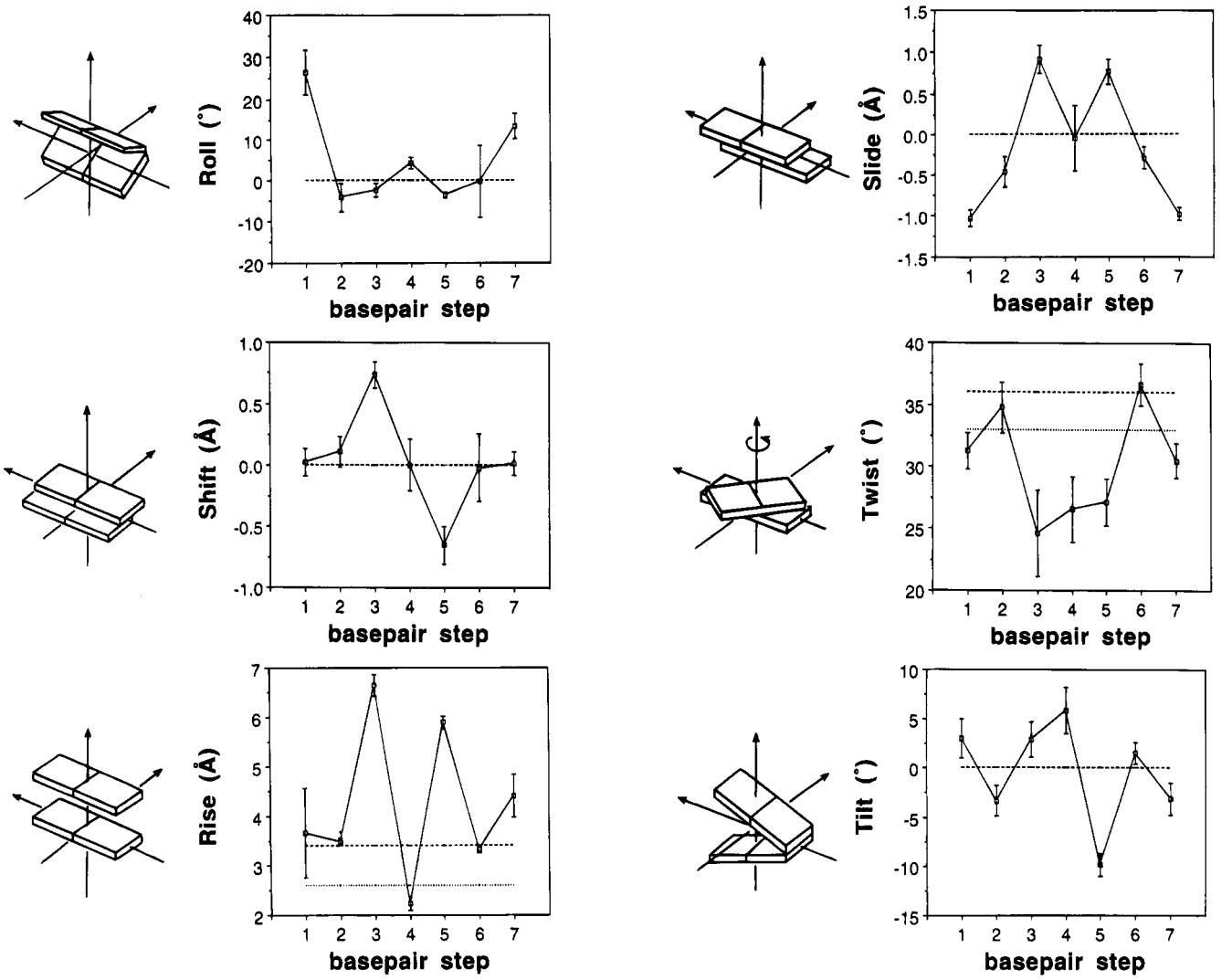

FIGURE 8: Helical parameters for the TOTO complex calculated using CURVES and compared with canonical A-DNA (···) and B-DNA (- - -).

compensate for each other. There are small deviations in the tilt (−10° to +15°) from the canonical B-form values. The helical twist changes in response to the intercalation of the TOTO chromophores. Intercalation causes unwinding at the intercalation site. The (G2-C3) and (G6-C7) base pair steps show the normal helical twist of 36°. The (C3-T4) and (A5-G6) base pair steps along with the central (T4-A5) step are underwound to ~25° in the complex. The helix is unwound by 60° and has an overall helical repeat of 12 base pairs in the complex, consistent with bis-intercalation of the TOTO. The distribution of the unwinding along the molecule is shown in Figure 8.

Comparison to Other Bis-Intercalators. TOTO belongs to a new structural class of "adaptable intercalators" in contrast to the common intercalators which bind in a parallel or perpendicular mode. Superficially, the intercalation of TOTO resembles the parallel mode of intercalation, but it can conform to the base pair propeller twist of the target dsDNA. This is all reflected in the slow on–off kinetics, the high binding constant, and the site selectivity.

The quinomycin antitumor antibiotics are a family of cyclic depsipeptides which bis-intercalate in dsDNA. Echinomycin is probably the best known among these compounds. Feigon and co-workers have studied the bis-intercalation of echinomycin in two different octamers and a decamer (Gilbert et al., 1989, 1991, 1992). They found that echinomycin bis-intercalates selectively on each side of a 5′-CpG-3′ site. Similar results have been found by Gao and Patel (1989). TANDEM, a fully synthetic compound, belongs to the triostin family of naturally occurring antibiotics that are closely related to quinomycins. While triostin and echinomycin show preference for 5′-CpG-3′-rich dsDNA, a methylated TANDEM analog preferentially binds to alternating 5′-TpA-3′ and 5′-CpI-3′ sequences (Addess et al., 1992; Addess & Feigon, 1994a,b). Luzopeptin is also a cyclic depsipeptide antibiotic that bis-intercalates in dsDNA. It has been shown that it binds by bracketing two AT base pairs (Searle et al., 1989). Common to the bis-intercalators of the quinomycin, triostin, and luzopeptin type is that the two intercalating chromophores are linked with cyclic peptide groups. The site selectivity of these compounds is predominantly ascribed to the interaction of this group with the dsDNA in the minor groove. Contributions to the site selectivity caused by the intercalating chromophore have not been described for these compounds.

Ditercalinium is a synthetic bis-intercalator with two rigid 7*H*-pyrido[4,3-*c*]carbazole chromophores linked together with an aliphatic piperidine-containing chain. An analog of ditercalinium has a more flexible spermine type of linker chain. In a series of papers, Delpierre and co-workers

(Delepierre et al., 1989a,b, 1991; Maroun et al., 1989; Pothier et al., 1991) have investigated the binding of these compounds to dsDNA of the size ranging from 4 to 8 base pairs. They concluded that the molecules bis-intercalate in the oligonucleotides with the chromophores preferentially in a 5′-CpG-3′ site and the linker chain in the major groove. While the conclusion with respect to the position of the linker chain is supported by an X-ray study (Williams & Gao, 1992), it is unclear to what extent the binding of ditercalinium to dsDNA is sequence selective. Most of the oligonucleotides used are short with only a few (or no) competing binding sites. Line broadening upon complex formation, due to dynamic exchange between different binding sites, makes spectral assignments difficult.

Comparison with ditercalinium supports the conclusion that the TOTO linker is a spectator in the sequence selectivity of this dye. The cationic chain contributes to the binding energy by van der Waals contacts, by Columbic attraction of the positively charged amino groups of the chain with the anionic phosphates of the dsDNA backbone. The positioning of the TOTO linker must be determined by the interaction of the chromophores with the bases of the dsDNA.

Site Selectivity. Our earlier NMR study (Jacobsen et al., 1995) showed that TOTO bis-intercalates in dsDNA with a considerable preference for a CTAG·CTAG site. We argued that this site selectivity is caused by the intercalating chromophores since the poly(propylenamine) linker was shown previously not to exhibit site selectivity by itself (Wemmer et al., 1985; Padmanabhan et al., 1988, 1991; Braunlin et al., 1982). Most other intercalating compounds show little site selectivity in the binding to various dsDNA oligonucleotides and when they do so, the effect is most convincingly explained as due to interactions of bulky side groups or linkers (Searle, 1993). The structure of the TOTO complex reveals that a characteristic feature of the TOTO chromophore is its ability to adapt to the base pair propeller twist of the dsDNA. Most other bis-intercalators have rigid aromatic chromophores that cannot adapt to the base pair propeller twist. This makes TOTO unique among bis-intercalators. The hydrophobic interaction between the thymidine methyl groups and the benzothiazole rings and stacking of the quinolinium ring with the purines probably provides significant contributions to the specific 5′-CpT-3′ site selectivity of TOTO.

Fluorescence Enhancement in the Complex. TOTO forms the kinetically most stable complex with dsDNA within the family of bis-intercalating dyes studied by Glazer and coworkers (Benson et al., 1993a,b). It is more stable than bis-(ethidium bromide). The fluorescence is enhanced by more than 3000 times upon binding to dsDNA.

Intercalation of the chromophores between the bases at the 5′-CpT-3′ step provides a possible explanation for the enhanced fluorescence of TOTO in the complex. Clamping of the TOTO chromophore between the dsDNA base pair prevents the free rotation of the benzothiazole ring about the C5−C6 bond relative to the quinolinium ring. This rotation is possible in uncomplexed TOTO, allowing relaxation nonradiatively. When bound to dsDNA the two halves of the chromophore are held much more rigidly together, and the chromophore loses excitation energy by fluorescence instead.

Biological Implications. The TOTO class of fluorescent bis-intercalators has been proven very effective in a variety of DNA detection applications. The finding of significant sequence specificity through interactions of the intercalating chromophore and the base pairs in this system was unexpected. This binding specificity will probably not interfere with its use as a general DNA stain, although there are situations where the binding preference could pose problems. With the high-resolution structure described here we have rationalized why TOTO exhibits sequence selectivity. The structure gives us the opportunity to try to manipulate the sequence selectivity of the dye. It will be possible to test the identified contributors to specificity by changing the DNA sequence and or modifying the ligand. Through further study of the structure it may be possible to identify new sites on the dye at which additional functional groups might make sequence-specific contacts.

There are many applications for sequence-specific dsDNA binding molecules both as drugs and as probes of dsDNA structure and function. Intercalation provides a large contact surface between the ligand and dsDNA which can provide a substantial free energy of binding. The combination of other binding motifs with an intercalative anchor has been exploited in both natural and synthetic systems. The sequence selectivity of these hybrid molecules was always determined by the nonintercalative part. Practical examples of this design concept include the addition of an intercalator to the end of a DNA strand designed to form a triplex and the linking of a minor groove ligand to an intercalator (Orson et al., 1994; Mouscadet et al., 1994; Bailly & Henichart, 1991; Subra et al., 1991; and references therein). The sequence specificity of the natural bis-intercalators (e.g., echinomycin) arises primarily from the interaction of the peptide linker with the dsDNA. Since the sequence specificity in TOTO arises from the interaction of the chromophore with the dsDNA, it may be possible to combine these motifs to achieve both higher affinity and specificity. Of course, attention must be paid to allow each of the components to obtain its optimum binding geometry without losing the advantage of linking them together. Another option is to combine the thiazole orange chromophore with other minor groove specific agents, such as netropsin. Such hybrid molecules could offer extended sequence recognition.

ACKNOWLEDGMENT

We are grateful to Professor A. Glazer, University of California, Berkeley, for providing TOTO. We are also grateful to Dr. F. Jensen and Dr. P. C. Stein, Department of Chemistry, Odense University, for setting up some of the computer programs and for many helpful discussions. We thank Professor T. L. James and Dr. H. Liu, University of California, San Francisco, for providing the MARDIGRAS and the RANDMARDI programs and for helpful guidelines. We also thank Dr. B. Geierstanger for carefully correcting the manuscript.

REFERENCES

Addess, K. J., & Feigon, J. (1994a) *Biochemistry 33*, 12386−12396.
Addess, K. J., & Feigon, J. (1994b) *Biochemistry 33*, 12397−12404.
Addess, K. J., Gilbert, D. E., Olsen, R. K., & Feigon, J. (1992) *Biochemistry 31*, 339−350.
Assa-Munt, N., Leupin, W., Denny, W. A., & Kearns, D. R. (1985a) *Biochemistry 24*, 1441−1449.
Assa-Munt, N., Leupin, W., Denny, W. A., & Kearns, D. R. (1985b) *Biochemistry 24*, 1449−1460.

Bailly, C., & Henichart, J. P. (1991) *Bioconjugate Chem. 2*, 379−393.
Bax, A., & Davis, D. (1985) *J. Magn. Reson. 65*, 355−360.
Benson, S. C., Singh, P. S., & Glazer, A. N. (1993a) *Nucleic Acids Res. 21*, 5727−5735.
Benson, S. C., Mathies, R. A., & Glazer, A. N. (1993b) *Nucleic Acids Res. 21*, 5720−5726.
Bodenhausen, G., Kogler, H., & Ernst, R. R. (1984) *J. Magn. Reson. 58*, 2161−2180.
Borgias, B. A., & James, T. L. (1990) *J. Magn. Reson. 87*, 475−487.
Borgias, B. A., Gochin, M., Kerwood, D. J., & James, T. L. (1990) *Prog. NMR Spectrosc. 22*, 83−100.
Braunlin, W. H., Strick, T. J., & Record, M. T., Jr. (1986) *Biopolymers 21*, 1301−1314.
Brown, T., & Brown, D. J. S. (1991) in *Oligonucleotides and Analogues. A Practical Approach* (Eckstein, F., Ed.) pp 1−23, Oxford University Press, Oxford.
Delepierre, M., Maroun, R., Garbay-Jaureguiberry, C., Igolen, J., & Roques, B. P. (1989a) *J. Mol. Biol. 210*, 211−228.
Delepierre, M., Dinh, T. H., & Roques, B. P. (1989b) *Biopolymers 28*, 2115−2142.
Delepierre, M., Mihle, C., Namane, A., Dinh, T. H., & Roques, B. P. (1991) *Biopolymers 31*, 331−353.
Dickerson, R. E., Bansal, M., Calladine, C. R., Diekermann, S., Hunter, W. N., Kennard, O., Lavery, R., Nelson, H. J. C., Saenger, W., Shakked, Z., Sklenar, H., Soumpasis, D. M., von Kitzing, E., Wang, A.-H., & Zhurkin, V. B. (1989) *EMBO J. 8*, 1−4.
Gao, X., & Patel, D. J. (1989) *Q. Rev. Biophys. 22*, 93−138.
Gilbert, D. E., & Feigon, J. (1991) *Biochemistry 30*, 2483−2494.
Gilbert, D. E., & Feigon, J. (1992) *Nucleic Acids Res. 20*, 2411−2420.
Gilbert, D. E., Van der Marel, G. A., Van Boom, J. H., & Feigon, J. (1989) *Proc. Natl. Acad. Sci. U.S. A. 86*, 3006−3010.
Hare, D. R., Wemmer, D. E., Chou, S.-H., Drobny, G., & Reid, B. R. (1983) *J. Mol. Biol. 171*, 319−336.
Jacobsen, J. P., Pedersen, J. B., Hansen, L. F., & Wemmer, D. E. (1995) *Nucleic Acids Res. 23*, 753−760.
Lavery, R., & Sklenar, H., (1988) *J. Biomol. Struct. Dynam. 6*, 63−91.
Lavery, R., & Sklenar, H. (1989) *J. Biomol. Struct. Dyn. 6*, 655−667.
Levitt, M., Freeman, R., & Frenkiel, T. (1982) *J. Magn. Reson. 47*, 328−330.
Maroun, R., Delepierre, M., & Roques, B. P. (1989) *J. Biomol. Struct. Dyn. 7*, 607−621.
Mouscadet, J. F., Ketterle, C., Goulaouic, H., Carteau, S., Subra, F., LeBret, M., & Auclair, C. (1994) *Biochemistry 33*, 4187−4196.
Orson, F. M., Kinsey, B. M., & McShan, W. M. (1994) *Nucleic Acids Res. 22*, 479−484.
Padmanabhan, S., Richey, B., Anderson, C. F., & Record, M. T., Jr. (1988) *Biochemistry 27*, 4367−4376.
Padmanabhan, S., Brushaber, V. M., Anderson, C. F., & Record, M. T., Jr. (1991) *Biochemistry 30*, 7550−7559.
Pothier, J., Delepierre, M., Barsi, M.-C., Garbay-Jaureguiberry, C., Igolen, J., Le Bret, M., & Roques, B. P. (1991) *Biopolymers 31*, 1309−1323.
Rye, R. S., Yue, S., Wemmer, D. E., Quesada, M. A., Haugland, R. P., Mathies, R. A., & Glazer, A. N. (1992) *Nucleic Acids Res. 20*, 2803−2812.
Rye, R. S., Dabora, J. M., Quesada, M. A., Mathies, R. A., & Glazer, A. N. (1993a) *Anal. Biochem. 208*, 144−150.
Rye, R. S., Yue, S., Quesada, M. A., Haugland, R. P., Mathies, R. A., & Glazer, A. N. (1993b) *Methods Enzymol. 217*, 414−431.
Searle, M. S. (1993) *Prog. NMR Spectrosc. 25*, 403−480.
Searle, M. S., Hall, J. G., Denny, W. A., & Wakelin, P. G. (1989) *Biochem. J. 256*, 433−441.
States, D. J., Haberkorn, R. A., & Reuben, F. J. (1982) *J. Magn. Reson. 48*, 286−292.
Stewart, J. J. P. (1993) *MOPAC 93.00 Manual*, Fujitsu Limited, Tokyo, Japan.
Subra, F., Carteau, S., Pager, J., Paoletti, J., Paoletti, C., Auclair, C., Mrani, D., Gosselin, G., & Imbach, J. L. (1991) *Biochemistry 30*, 1642−1650.
Wemmer, D. E., Srivenugopal, K. S., Reid, B. R., & Morris, D. R. (1985) *J. Mol. Biol. 185*, 457−459.
Williams, L. D., & Gao, Q. (1992) *Biochemistry 31*, 4315−4324.
Wüthrich, K. (1986) *NMR of proteins and nucleic acids*, John Wiley & Sons, New York.

BI950034X